

Structure of vortices in a Karman street behind a heated cylinder

A. B. Ezersky,¹ J. C. Lecordier,² P. Paranthoën,² and P. L. Soustov¹

¹*Institute of Applied Physics, Russian Academy of Science, 46 Uljanov Street, 603600 Nizhny Novgorod, Russia*

²*Université de Rouen, CNRS UMR No. 6614, 76821 Mont Saint Aignan Cedex, France*

(Received 10 February 1999)

The velocity and temperature fields in a wake behind a heated cylinder are investigated for Reynolds numbers in the interval $65 < \text{Re} < 110$. Spatial distributions of the amplitudes and phases of the first harmonics of velocity and temperature fluctuations in the region of formation of a vortex street are determined. A simple kinematic model is constructed to explain the evolution of the phase difference of the first harmonics of velocity and temperature fluctuations with increasing distance from the cylinder.

PACS number(s): 47.27.Vf, 47.27.Te, 47.32.Cc

A vortex street behind a heated cylinder is a classical object for investigation of heat transfer in flows. Until recently, investigations of a flow around a heated cylinder and of heated bodies in general were focused on the dependence of averaged characteristics of heat transfer (e.g., Nusselt number) on Reynolds number and on other flow parameters: degree of turbulence, roughness, and cylinder elongation. For the control of heat transfer detailed information about velocity and temperature fields in wakes behind heated bodies is needed. The most complete investigation of the structure of heat transporting vortices was carried out for large Reynolds numbers $\text{Re} \sim 10^3$ (see, e.g., Ref. [1]), when the vortex street is turbulent. The use of various averaging methods for processing results of measurements of velocity and temperature fluctuations at different points enabled researchers to clarify the structure of the fields and determine the vortex regions that transport heat most effectively. Such a research, as far as we know, was not done for the laminar street ($\text{Re} \leq 10^2$). It is important to clarify what the velocity and temperature fields are at the Reynolds numbers corresponding to a laminar Karman street. Of particular interest are processes in the region of formation of a vortex street, at a distance from the cylinder of about several tens of its diameter. These problems will be considered in the present paper.

Fluctuating velocity and temperature fields were analyzed using spectral analysis of time series. As was mentioned in Ref. [2], the major portion of energy is concentrated at the fundamental harmonic. Consequently, in our measurements we recorded amplitude and phase characteristics of the fundamental frequency (Strouhal frequency) of velocity and temperature fluctuations. Note that such measurements in the interval of Reynolds numbers $65 < \text{Re} < 110$ were not carried out before. Either root-mean-square velocity or temperature averaged over time were measured as a rule. The point is that velocity fluctuations in the presence of temperature fluctuations at small flow velocities are usually measured by laser Doppler anemometer [2], and it is difficult to obtain a continuous signal needed for spectral analysis and for measurement of the phases of harmonics. In our measurements we employed hot wire anemometers and temperature bridges that enabled us to obtain signals continuous in time.

Experiments were performed in a flow that was a plane horizontal air jet having a cross section of $15 \times 150 \text{ mm}^2$. A streamlined cylinder 1 mm in diameter having the length $L = 150 \text{ mm}$ was placed horizontally in the middle of the jet (Fig. 1). The cylinder was heated by Joule effect by means of direct current. The heat input per unit length was calculated from the supplied voltage and current. The jet was controlled by a microanemometer and the temperature of the cylinder was measured by means of a thermocouple located within the tube. The cylinder was heated from the inside by means of a Ni-Cr wire carrying direct current. The wire temperature was controlled by a thermocouple. The fluctuations of the longitudinal velocity component were measured by means of a DISA hot wire anemometer system, and temperature fluctuations by a specially designed bridge. Both the temperature and the velocity fluctuations were measured by a transducer made of a platinum filament $1.2 \mu\text{m}$ in diameter. When operated with the DISA it acted as a velocity transducer, and with the bridge as a temperature transducer. Strictly speaking, for a flow containing both temperature and velocity fluctuations, the signal from hot wire anemometer is a mixture of these components. In this connection we carried out measurements that allowed us to determine the temperature range of a streamlined cylinder and the power density at which the contribution of temperature fluctuations may be neglected in measurements of velocity fluctuations (the velocity fluctuations were measured to an accuracy of 10% and higher). For determination of fluctuation spectra and for phase measurements we employed an FFT 1201 double-

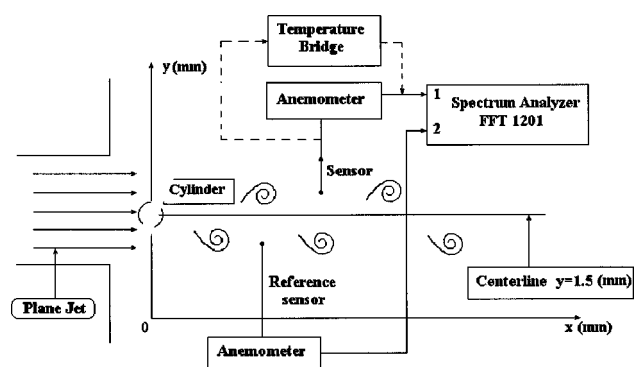


FIG. 1. Experimental setup.

channel spectrum analyzer. The phase difference was calculated in the regime for determining signal cross spectrum. The cross spectrum of two variables $V(t), T(t)$ is defined by

$$S_{V,T}(f) = \hat{V}(f)\hat{T}^*(f) = |\hat{V}(f)||\hat{T}(f)|e^{i[\hat{\Phi}_V(f) - \hat{\Phi}_T(f)]}. \quad (1)$$

Here, $\hat{V}(f), \hat{T}(f)$ are the components of the Fourier spectra of variables $V(t), T(t)$ and an asterisk denotes a complex conjugate quantity. Phase measurements were conducted by means of a reference transducer (see Fig. 1). Cross spectra were measured in the frequency range of 0 to 1000 Hz using averaging over 100 time series without overlap. We first recorded the reference-signal-velocity-fluctuation cross spectrum, as the velocity transducer was moved across the jet, and determined phase distribution. Then, the same transducer was connected to the temperature bridge and, at the same coordinates, the reference-signal-temperature-fluctuation cross spectrum was measured. From these cross spectra we determined the phase difference of the fundamental frequencies of temperature and velocity.

The measurements verified that the amplitudes of the fundamental harmonics of velocity and temperature fluctuations initially increased downstream and then decayed. The behavior of the amplitude of the fundamental harmonic of velocity fluctuations was very similar to that of the velocity fluctuations measured in Ref. [2]. The measurements of cross spectra allowed us to obtain the phase difference between the first harmonics of velocity and temperature fluctuations. It was found that for harmonics with the amplitudes exceeding the level of noise by more than 15 dB we had a well defined phase the value of which is approximately equal for all components in the neighborhood of the spectral peak. The use of cross spectra enabled us to determine the phases of the fundamental harmonics of velocity and temperature and the phase difference at different Reynolds numbers and at different distances from the cylinder [Figs. 2(a)–2(c)]. Apparently, the phases of the fundamental harmonics are determined to an accuracy of additive constant (the phase of the reference signal), whereas the reference signal phase is excluded in determining the phase difference. Phase measurements were correct only in the region of sufficiently high amplitudes of fundamental harmonics. In the middle of the street, where the second harmonic is higher than the first one, and at the periphery, where the amplitudes of all harmonics are small, the phases were determined in error and are not shown in Fig. 2. The maxima of velocity and temperature fluctuations in this figure are in the intervals $0.2 \text{ mm} < y < 0.5 \text{ mm}$ and $2.5 \text{ mm} < y < 2.8 \text{ mm}$, the centerline of the Karman street corresponds to $y = 1.5 \text{ mm}$.

It is clear from Fig. 2 that velocity and temperature fluctuations near the cylinder ($x = 5$) obey a quadratic law: the phase difference of the first harmonics of fluctuations of vortex motion is about 90° . This means that, at a distance of several diameters, vortices in a Karman street almost do not transport heat in the longitudinal direction. Mean flow makes the principal contribution to heat transfer. With increasing distance from the cylinder, the phase difference of the harmonics reduces and heat transport by fluctuation components $\langle uT \rangle$ in the longitudinal direction is intensified.

In an effort to explain the dependences of phase differences of the fundamental frequencies we take a simple kine-

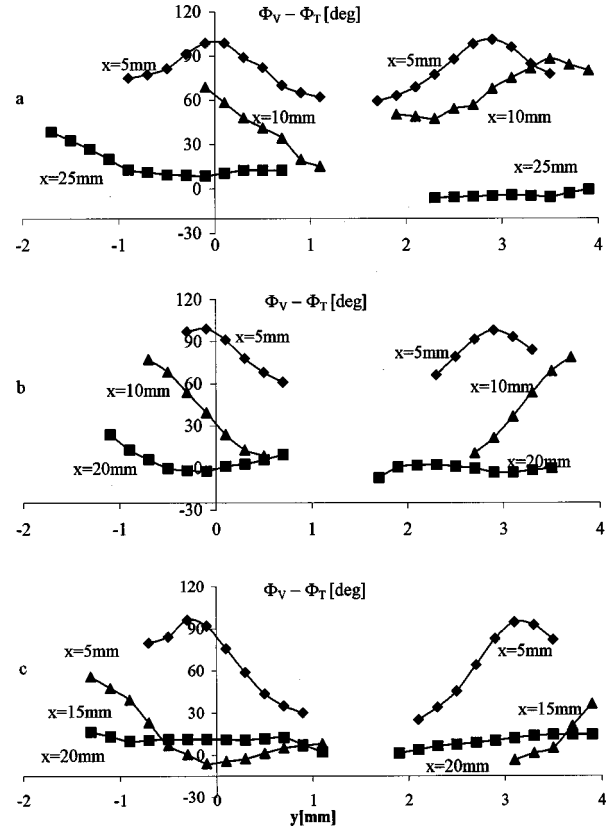


FIG. 2. The phase differences of the first harmonics of velocity and temperature fluctuations versus transverse coordinate at different distances from the cylinder: (a) $Re=65$, $P/L=2.4 \text{ W/m}$ for $x = 5 \text{ mm}$ ($5d$), $x = 10 \text{ mm}$ ($10d$), etc. (b) $Re=90$, $P/L=4 \text{ W/m}$; (c) $Re=110$, $P/L=7 \text{ W/m}$.

matic model. Evidently, the most consistent approach is the calculation of Navier-Stokes equations supplemented by equations for heat transfer. We believe that basic regularities revealed in experiment may be explained on a simple physical model. We suppose that the vortex Karman street (velocity field) has been formed and calculate transport of passive contaminant (temperature) in such a vortex street. We regard the vortex street as two rows of nonpoint vortices arranged in chess order. Vorticity distribution inside a circle of radius r_0 has the form

$$\Omega = \Omega_0 \frac{\cos[\pi(r/r_0)] + 1}{2}, \quad (2)$$

where r_0 is the characteristic radius of the vortex and Ω_0 is constant vorticity.

Similar models of Karman street were developed in Ref. [4], where data obtained by means of hot wire anemometers and by vortex visualization were compared.

Outside the circle of radius $r=r_0$, the vortices are potential and the velocity field in this region does not differ from that at superposition of point vortices. Note that the velocity field \vec{V} of the vortex street is given (stability of such vortices is not considered here), and we investigate diffusion and heat transport in the given field.

Under the suppositions made above, the temperature field obeys the following dimensionless equation:

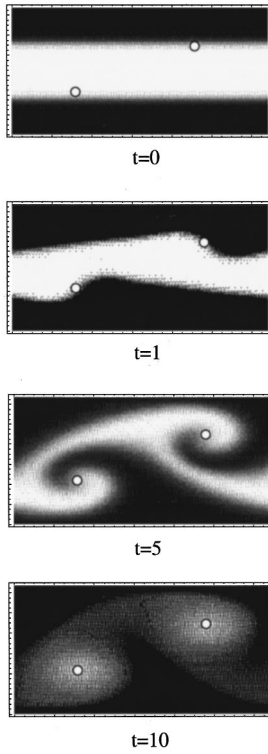


FIG. 3. Evolution of the temperature field: image brightness is proportional to temperature, circles correspond to the positions of vortex cores.

$$\frac{\partial T}{\partial t} + \frac{1}{\alpha v^*} \vec{v} \nabla T = \frac{1}{\beta \alpha^2 P \text{Re} v^*} \Delta T. \quad (3)$$

Here, t is the dimensionless time normalized to the repetition rate of vortices t_v ;

$$\nabla = \left(\frac{\partial}{\partial x} \vec{x}_0 + \frac{\partial}{\partial y} \vec{y}_0 \right), \quad \Delta = \frac{\partial^2}{\partial x^2} + \frac{\partial^2}{\partial y^2},$$

where x and y are the dimensionless coordinates normalized to the vortex street width h ; $\vec{v} = \vec{V}/U_0$, U_0 being the velocity of the incident flow; $\alpha = h/l$, l is the spatial period of vortex street; \vec{v}^* is the velocity of the vortex street (in the coordinate system in which a cylinder is at rest) normalized to U_0 ; $\text{Re} = U_0 d/\nu$ is the Reynolds number (ν being kinematic viscosity of the air, and d diameter of the cylinder); $\beta = 1/d = \beta(\text{Re})$ is the empiric coefficient relating the vortex street period to diameter; and $P = \nu/\kappa$ is the Prandtl number.

The evolution of the temperature field was calculated for the region with periodic boundary conditions for the x coordinate (see Fig. 3)

$$T(x, y, t) = T(x + l, y, t) \quad (4)$$

and zero temperature gradient at a large distance from the centerline of vortex street for the y coordinate

$$\frac{\partial T(x, 0, t)}{\partial y} = \frac{\partial T(x, 3h, t)}{\partial y} = 0. \quad (5)$$

Here, $y=0$ and $y=3$ are the vertical boundaries of the region for which numerical calculation is performed. The

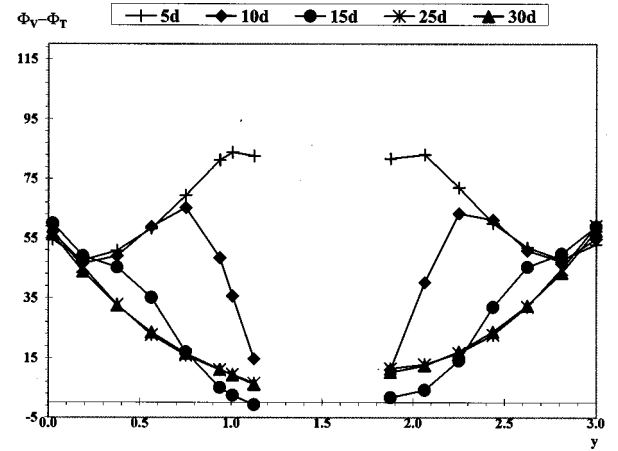


FIG. 4. The phase differences of the first harmonics of velocity and temperature fluctuations versus transverse coordinate at different distances from the cylinder. Results of numerical experiment for $\text{Re}=90$.

initial temperature distribution and time evolution of the temperature are plotted in Fig. 4. It is clearly seen in this figure that the heated gas is concentrated in the vortex cores. Apparently, the maximal temperature in the vortex cores drops in the course of time due to diffusion, but it is still much higher than the temperature at the periphery of the vortex street.

We will compare evolution of the temperature field in time with its evolution in space along the x coordinate, bearing in mind that one space period corresponds to one time period. The space period of Karman street in the range of Reynolds numbers under investigation is equal approximately to $5d$, so in our figures we present results of numerical calculations and experimental research for distances multiple to this value.

Using numerical simulation we determined the distribution of the phases of the fundamental harmonics of temperature and velocity fluctuations in the transverse direction that has a good qualitative agreement with results of experiments. In particular, for fundamental harmonics the model includes phase jumps equal to π across the centerline $y=1.5$.

The phase difference of the first harmonics of temperature and velocity fluctuations within the proposed model for $\text{Re}=90$ is presented in Fig. 4. The phase difference is about 90° at the initial stage ($x \sim 5d$). Further, the heated gas is concentrated in the vortex cores and the phase difference drops down to 5° – 10° . However, the phase difference is nonzero at the periphery of the street where the amplitudes of temperature and velocity fluctuations are small. Similar dependences were observed for $\text{Re}=65$ and $\text{Re}=100$.

Comparison of experimental and theoretical results allows us to formulate conclusions. It was shown in Ref. [3] that heating of a cylinder streamlined by air decreases the vortex shedding frequency. This means that temperature cannot be regarded as a passive contaminant. The temperature influences the medium viscosity and, as a consequence, the mean flow profile and the vortex shedding frequency [3]. However, calculations and comparison with experiment show that, for fluctuation components, temperature may be regarded as a passive contaminant. Under the assumption that the temperature field is transported by the Karman street (vortices in-

volve in motion liquid particles from a warm wake the temperature of which is higher than that of the incident flow) one obtains rather good agreement with experiment. It should be emphasized that we used in numerical calculations a stationary field of velocity and were not concerned with the influence of temperature field on stability of the Karman street. We took into account only the temperature field transport by a vortex flow and diffusion of the temperature field. A purely kinematic model enables one to explain not only the trans-

verse amplitude profiles observed in experiment but also more delicate characteristics, such as the dependence of the phase difference of the first harmonics of temperature and longitudinal velocity fluctuations along the transverse coordinate.

One of the authors (E. A. B.) highly appreciates the offered opportunity to work as a visiting professor at the UMP 6614 CNRS laboratory of Rouen University where the experimental data presented above were obtained.

[1] M. Matsumura and R. A. Antonia, *J. Fluid Mech.* **250**, 651 (1993).

[2] J. E. Westfreid *et al.*, *J. Phys. II* **6**, 1343 (1996).

[3] J. C. Lecordier *et al.*, *Exp. Fluids* **10**, 224 (1991).

[4] M. Okude and T. Matsui, *Trans. J. Soc. Aero. Space Sci* **30**, 80 (1987); **33**, 1 (1990).